Molecular Pharmacology Fast Forward. Published on May 20, 2015 as DOI: 10.1124/mol.114.097345
This article has not been copyedited and formatted. The final version may differ from this version.

Identification of a dual inhibitor of SRPK1 and CK2 that attenuates pathological angiogenesis of macular degeneration in mice

Satoshi Morooka, Mitsuteru Hoshina, Isao Kii, Takayoshi Okabe, Hirotatsu Kojima, Naoko Inoue, Yukiko Okuno, Masatsugu Denawa, Suguru Yoshida, Junichi Fukuhara, Kensuke Ninomiya, Teikichi Ikura, Toshio Furuya, Tetsuo Nagano, Kousuke Noda, Susumu Ishida, Takamitsu Hosoya, Nobutoshi Ito, Nagahisa Yoshimura, Masatoshi Hagiwara

Department of Ophthalmology and Visual Sciences (S.M., N.Y.), Department of Anatomy and Developmental Biology (S.M., I.K., K.N., M.H.), and Medical Research Support Center (Y.O., M.D.), Graduate School of Medicine, Kyoto University, Kyoto, Japan; Laboratory of Structural Biology, Medical Research Institute (M.H., T.I., N.I.), and Laboratory of Chemical Bioscience, Institute of Biomaterials and Bioengineering (S.Y., T.H.), Tokyo Medical and Dental University, Tokyo, Japan; Open Innovation Center for Drug Discovery, The University of Tokyo, Tokyo, Japan (T.O., H.K., T.N.);

Downloaded from molpharm.aspetjournals.org at ASPET Journals on April 19, 2024

Molecular Pharmacology Fast Forward. Published on May 20, 2015 as DOI: 10.1124/mol.114.097345
This article has not been copyedited and formatted. The final version may differ from this version.

PharmaDesign, Inc, Tokyo, Japan (N.I., T.F.); Department of Ophthalmology, Graduate School of Medicine, Hokkaido University, Sapporo, Japan (J.F., K.N., S.I.)

Downloaded from molpharm.aspetjournals.org at ASPET Journals on April 19, 2024

Molecular Pharmacology Fast Forward. Published on May 20, 2015 as DOI: 10.1124/mol.114.097345
This article has not been copyedited and formatted. The final version may differ from this version.

Identification of an anti-angiogenic inhibitor of SRPK1 and CK2

Address correspondence to:

Masatoshi Hagiwara, Department of Anatomy and Developmental Biology, Graduate School of Medicine, Kyoto University, Yoshida-Konoe-cho, Sakyo-ku, Kyoto 606-8501, Japan.

Tel: +81-75-753-4341 and Fax: +81-75-751-7529

E-mail: hagiwara.masatoshi.8c@kyoto-u.ac.jp

Text pages: 1- 48

Figures: 1-6

References: 64

The number of words in the *Abstract*: 159

The number of words in the *Introduction*: 512

The number of words in the *Discussion*: 860

Downloaded from molpharm.aspetjournals.org at ASPET Journals on April 19, 2024

Molecular Pharmacology Fast Forward. Published on May 20, 2015 as DOI: 10.1124/mol.114.097345
This article has not been copyedited and formatted. The final version may differ from this version.

Abbreviations

VEGF: vascular endothelial growth factor

SRPK1: serine-arginine protein kinase 1

CK2: casein kinase 2

AMD: age-related macular degeneration

DMSO: dimethyl sulfoxide

HIF1: hypoxia-inducible factor-1

MCP1: monocyte chemoattractant protein-1

ICAM1: intercellular adhesion molecule-1

ANOVA: analysis of varance

Downloaded from molpharm.aspetjournals.org at ASPET Journals on April 19, 2024

Molecular Pharmacology Fast Forward. Published on May 20, 2015 as DOI: 10.1124/mol.114.097345
This article has not been copyedited and formatted. The final version may differ from this version.

Abstract

Excessive angiogenesis contributes to numerous diseases, including cancer and blinding retinopathy. Antibodies against vascular endothelial growth factor (VEGF) have been approved, and are widely used in the clinical treatment. Our previous studies using SRPIN340, a small molecule inhibitor of SRPK1 (Serine-Arginine Protein Kinase 1), demonstrated that SRPK1 is a potential target for development of anti-angiogenic drug. In this study, we solved the structure of SRPK1 bound to SRPIN340 by X-ray crystallography. Using pharmacophore docking models followed by *in vitro* kinase assays, we screened a large-scale chemical library, and thus identified a new inhibitor of SRPK1. This inhibitor, SRPIN803, prevented VEGF production more effectively than SRPIN340 due to the dual inhibition of SRPK1 and CK2 (Casein Kinase 2). In a mouse model of age-related macular degeneration, topical administration of eye ointment containing SRPIN803 significantly inhibited choroidal neovascularization, suggesting a clinical potential of SRPIN803 as a topical ointment for ocular neovascularization. Thus SRPIN803 merits further investigation as a novel inhibitor of VEGF.

Downloaded from molpharm.aspetjournals.org at ASPET Journals on April 19, 2024

Molecular Pharmacology Fast Forward. Published on May 20, 2015 as DOI: 10.1124/mol.114.097345
This article has not been copyedited and formatted. The final version may differ from this version.

Introduction

Angiogenesis is an important biological phenomenon, not only in physiological conditions including embryogenesis, skeletal growth, and wound healing, but also in pathological conditions such as tumor growth, chronic inflammatory disorders, and intraocular neovascular diseases (Maharaj and D'Amore, 2007). VEGF, a mitogen for endothelial cells, is a key regulator of angiogenesis associated with various pathological conditions (Ferrara et al., 2003; Okabe et al., 2014). VEGF binds VEGF receptor and activates its tyrosine kinase activity, which in turn triggers the MAPK signaling cascade (Fukuda et al., 2002), leading to endothelial cell proliferation and neovascularization (Xu et al., 2008). Because of the importance of VEGF in these processes, drugs targeting VEGF have been developed: for example, an antibody against VEGF, bevacizumab (Avastin), was first approved for patients with metastatic colorectal cancer (Hurwitz et al., 2004). Anti-VEGF antibodies have the potential to be of therapeutic value for a variety of angiogenic disorders.

Anti-VEGF antibodies, including ranibizumab (Lucentis) (Rosenfeld et al., 2006), pegaptanib (Macugen) (Gragoudas et al., 2004), and anti-VEGF decoy receptor of

Downloaded from molpharm.aspetjournals.org at ASPET Journals on April 19, 2024

Molecular Pharmacology Fast Forward. Published on May 20, 2015 as DOI: 10.1124/mol.114.097345
This article has not been copyedited and formatted. The final version may differ from this version.

aflibercept (Eylea) (Heier et al., 2012), have also approved for intraocular neovascularization. Age-related macular degeneration (AMD) is one of the most common diseases of intraocular neovascularization, the leading cause of blindness (Ferris et al., 1984; Klein et al., 1995; Seddon and Chen, 2004). Intravitreous injection of anti-VEGF antibodies has been demonstrated to cure AMD; however, this therapy increases the risk of several complications including infection, inflammation, higher intraocular pressure, and vitreous hemorrhage (Shima et al., 2008; Ventrice et al., 2013). Therefore, there is an urgent need for new therapeutics based on small molecules that can be safely and easily administered, such as eye drops and ointments. Small-molecule inhibitors of angiogenesis would also contribute to therapies against other angiogenic diseases.

In a previous study, we demonstrated the anti-angiogenic activity of SRPIN340, a small molecule that was developed as an inhibitor of SRPK1 (Fukuhara et al., 2006). SRPK1 phosphorylates serine/arginine-rich proteins and regulates splicing and transcription (Ngo et al., 2005; Nishida et al., 2011; Ogawa and Hagiwara, 2012), and also phosphorylates PGC1, hepatitis B virus core protein, and eIF4G to regulate

Downloaded from molpharm.aspetjournals.org at ASPET Journals on April 19, 2024

Molecular Pharmacology Fast Forward. Published on May 20, 2015 as DOI: 10.1124/mol.114.097345
This article has not been copyedited and formatted. The final version may differ from this version.

glucogenesis (Lin et al., 2005; Nikolakaki et al., 2008), viral replication (Daub et al., 2002), and mTOR signaling (Hu et al., 2012), respectively. SRPK1 inhibition prevents pathological angiogenesis, and suppresses angiogenesis-associated tumor growth (Amin et al., 2011) and pathological choroidal neovascularization in animal models (Dong et al., 2013). Inversely, aberrant SRPK1 expression induces constitutive Akt activation, leading to cancer progression (Wang et al., 2014). Thus, SRPK1 represents a potent drug target for treatment of pathological angiogenesis.

Here, we report the application of a computational protocol based on molecular docking and dynamics simulations, combined with a pharmacophore-based database search, to identify hit compounds. Using this method, we identified a new small molecule, SRPIN803, that inhibits VEGF production. *In vitro* kinase profiling revealed that SRPIN803 inhibited CK2 as well as SRPK1. The dual inhibition of SRPK1 and CK2 were predicted to synergistically suppress VEGF production. In a mouse model, topical administration of SRPIN803 suppressed intraocular neovascularization. Thus, SRPIN803 represents a candidate therapeutic drug for treatment of pathological angiogenesis.

Downloaded from molpharm.aspetjournals.org at ASPET Journals on April 19, 2024

Molecular Pharmacology Fast Forward. Published on May 20, 2015 as DOI: 10.1124/mol.114.097345
This article has not been copyedited and formatted. The final version may differ from this version.

Materials and Methods

Crystallographic study

Crystals of the kinase fragment of SRPK1 (residues 42–255 and 474–655) were obtained according to a previously reported method (Ngo et al., 2007) with some modifications. The SRPIN340 complex was obtained by soaking crystals of apo-SRPK1 in mother liquor containing the inhibitor.

The diffraction data set was obtained at 100 K from a single crystal at BL38B1 of SPring-8 (Harima, Japan). The 2.0-Å diffraction data were integrated and scaled using the program HKL2000 (HKL Research Inc., Charlottesville, VA). The space group was $P6_522$, with unit cell parameters $a = b = 75.1$ Å and $c = 310.6$ Å.

Structure determination and refinement were performed using the CCP4 suite (Winn et al., 2011). The structure was solved by molecular replacement using a previously reported structure of SRPK1 (PDB ID: 1WAK; (Ngo et al., 2007)) and refined by REFMAC (Murshudov et al., 2011). The graphics software Coot was used for model-building (Emsley et al., 2010). Some of the statistics of data collection and structure refinement are shown in Supplemental Table 1. Figures were created using the PyMOL Molecular

Downloaded from molpharm.aspetjournals.org at ASPET Journals on April 19, 2024

Molecular Pharmacology Fast Forward. Published on May 20, 2015 as DOI: 10.1124/mol.114.097345
This article has not been copyedited and formatted. The final version may differ from this version.

Graphics System (Version 1.5.0.4, Schrödinger, LLC). Coordinates and structure factors of the complex were deposited in the Protein Data Bank (PDB ID: 4WUA).

Docking simulation

The model of the SRPIN803 in complex with CK2α was obtained using AutoDock Vina (Trott and Olson, 2010). The crystal structure of the inhibitor complex of CK2α (PDB ID: 1M2Q; (De Moliner et al., 2003)) was used as the protein model after removal of the ligand and inhibitor molecules. The docking simulation was performed around the ATP-binding pocket of CK2α. The model of SRPIN803 in complex with SRPK1 was obtained in a similar manner, using our X-ray structure as the protein model. The coordinates of the models can be found in the Supplemental Data. The result was visualized using Discovery Studio Visualizer (Accelrys Inc., Cambridge, UK).

Cell culture

ARPE-19 cells, a spontaneously arising human retinal pigment epithelia cell line, were purchased from ATCC, and maintained at 37°C in a 5% CO_2/air incubator in Dulbecco's

Downloaded from molpharm.aspetjournals.org at ASPET Journals on April 19, 2024

Molecular Pharmacology Fast Forward. Published on May 20, 2015 as DOI: 10.1124/mol.114.097345
This article has not been copyedited and formatted. The final version may differ from this version.

modified Eagle's medium (DMEM)/Ham's F-12 (Nacalai Tesque, Kyoto, Japan) supplemented with 10% fetal bovine serum (Sigma-Aldrich, St. Louis, MO) and 1% Penicillin–Streptomycin Mixed Solution (Nacalai Tesque).

siRNA

Stealth siRNAs (Life technologies, Inc., Gaitherburg, MD) were diluted with OptiMEM (Life Technologies, Inc.), and incubated with Lipofectamine RNAiMAX (Life Technologies, Inc.). ARPE-19 cells were seeded onto 12-well plates at 50,000 cells/well, and then transfected with siRNAs (final concentration, 10 nM) against *SRPK1*, *CK2A1*, *CK2A2*, or *Luciferase*. Analyses were performed 48 hours post-transfection. Product names of the siRNAs used were as follows: *SRPK1* (SRPK1-HSS110210), *CK2A1* (CSNK2A1-HSS175396), *CK2A2* (CSNK2A2-HSS102398), and Luciferase (Life Technologies, Inc.).

Reverse transcription and semi-quantitative and quantitative PCR

Total RNA was purified from cells using the RNeasy kit (QIAGEN, Hilden, Germany).

Downloaded from molpharm.aspetjournals.org at ASPET Journals on April 19, 2024

Molecular Pharmacology Fast Forward. Published on May 20, 2015 as DOI: 10.1124/mol.114.097345
This article has not been copyedited and formatted. The final version may differ from this version.

Purified RNA was converted into cDNA using SuperScript II (Life Technologies, Inc.) with anchored oligo-dT primer (Life Technologies, Inc.).

Ex Taq (TaKaRa Bio, Otsu, Japan) was used for semi-quantitative PCR analysis. The reaction was carried out using the following cycle: 95°C for 20 seconds, 58°C for 20 seconds, and 72°C for 60 seconds, for 25–35 cycles. Primer sequences are listed in Supplemental Table S5. PCR products were separated by electrophoresis and stained with ethidium bromide (Nacalai Tesque). Images were obtained using a ChemiDoc XRS System (Bio-Rad Laboratories, Hercules, CA).

Quantitative PCR was performed using SYBR Premix Ex Taq (TaKaRa Bio) on a real-time PCR cycler (StepOnePlus, Life Technologies, Inc.). The human *GAPDH* gene was used to normalize the input cDNA. Sequences of the primers are listed in Supplemental Table 6. All cDNA samples were tested in duplicate, and the average values were used in statistical analysis.

Enzyme-Linked Immunosorbent Assay (ELISA)

ARPE-19 cells were seeded at a density of 1×10^4 cells/well in 12-well plates and

Downloaded from molpharm.aspetjournals.org at ASPET Journals on April 19, 2024

Molecular Pharmacology Fast Forward. Published on May 20, 2015 as DOI: 10.1124/mol.114.097345
This article has not been copyedited and formatted. The final version may differ from this version.

cultured for 24 hours. The culture medium was replaced with DMEM supplemented with 1% FBS 24 hours before treatment with compounds. The cells were treated with 1 nM TGFβ (R&D Systems, Minneapolis, MN). Culture supernatants were collected 24 hours or 72 hours after the treatment, and VEGF levels in the supernatants were determined using an ELISA kit (R&D Systems).

***In vitro* kinase assay**

Recombinant human SRPK1 protein was purified from *E. coli* (Fukuhara et al., 2006). The *in vitro* kinase assay was performed as described previously (Fukuhara et al., 2006) with some modifications. The SRPK1 kinase reaction was performed in a reaction mixture containing serially diluted inhibitors, 10 mM MOPS-KOH (pH 7.0), 10 mM magnesium acetate, 200 μM EDTA, 1 μM ATP, 0.017 mg/mL RS peptide, and recombinant SRPK1 in a final volume of 25 μL. The final concentration of DMSO was adjusted to 0.1% or 1%, regardless of the inhibitor concentration.

Human recombinant casein kinase 2 (CK2) was purchased from New England Biolabs. The CK2 kinase reaction was performed in a reaction mixture containing serially

Downloaded from molpharm.aspetjournals.org at ASPET Journals on April 19, 2024

Molecular Pharmacology Fast Forward. Published on May 20, 2015 as DOI: 10.1124/mol.114.097345
This article has not been copyedited and formatted. The final version may differ from this version.

diluted inhibitors, 20 mM Tris-HCl (pH 7.5), 50 mM potassium chloride, 10 mM magnesium chloride, 20 μM ATP, 0.02 mg/mL CK2 substrate (Sigma-Aldrich), and 625 U of recombinant CK2 in a final volume of 25 μl. The final concentration of DMSO was adjusted to 1%, regardless of the inhibitor concentration.

The reaction mixture was incubated at 30°C for 15 min, and residual ATP was measured using Kinase-Glo (Promega).

Relative kinase Activity (%) = (C – A) / (C – B) × 100

A: Count per second (CPS) from the reaction with an inhibitor

B: CPS from the reaction with 1% DMSO

C: CPS from the reaction without enzyme (background)

Laser-induced choroidal neovascularization in mice

All animal experiments were approved by the Kyoto University Animal Use Committee and conducted in accordance with the Association for Research in Vision and Ophthalmology Statement for the Use of Animals in Ophthalmic and Vision Research. Six- to eight-week-old C57BL/6J male mice (Japan SLC, Tokyo, Japan) were used for

Downloaded from molpharm.aspetjournals.org at ASPET Journals on April 19, 2024

Molecular Pharmacology Fast Forward. Published on May 20, 2015 as DOI: 10.1124/mol.114.097345
This article has not been copyedited and formatted. The final version may differ from this version.

this study. Anesthesia was induced by intraperitoneal injection of ketamine (100 mg/kg body weight) and xylazine (10 mg/kg body weight), and pupils were dilated by topical administration with 5% phenylephrine hydrochloride and 5% tropicamide. After anesthesia and pupil dilation, four laser spots were placed around the optic disc (532 nm, 150 mW power, 0.1 seconds, spot size 75 μm in diameter; Novus Spectra, Lumenis, Tokyo, Japan) using a slit-lamp delivery system with a cover glass as a contact lens.

Intravitreous injection

Each compound (50 mM in DMSO) was diluted with PBS to various concentrations (final 0.1% DMSO) just before injection. Immediately after laser photocoagulation, 1.0 μL of the diluted solution was injected into the vitreous body using a 33-gauge needle (Extreme Microsyringe, Ito Corporation, Tokyo, Japan).

Administration of the ointment

SRPIN803 was formulated into an ointment base containing fluid paraffin and white Vaseline to a final concentration of 10%. The ointment base alone was used as a negative

Downloaded from molpharm.aspetjournals.org at ASPET Journals on April 19, 2024

Molecular Pharmacology Fast Forward. Published on May 20, 2015 as DOI: 10.1124/mol.114.097345
This article has not been copyedited and formatted. The final version may differ from this version.

control. These ointments were partitioned into 1.5 mL tubes, and stored in the dark at room temperature. The ointment (7.0 μL) was applied to both eyes of the model mice, three times per day for 7 days, using a Microman (Gilson, Middleton, WI).

Measurement of the neovascularization area

Seven days after laser-induced photocoagulation, model mice were euthanized by anesthesia and perfused with 1 mL of 0.5% fluorescein isothiocyanate–labeled dextran (Sigma-Aldrich). Flat mounts of retinal pigment epithelium and choroid were obtained by removing the anterior segments and the neural retina. Four to six radial relaxing incisions were made to allow the residual posterior eyecup to be laid flat. After mounting with Aqua-Poly/Mount (Polysciences, Warrington, PA) and coverage with a coverslip, the flat mounts were examined with a fluorescence microscope (Biorevo BZ-9000, Keyence, Osaka, Japan), and the area of neovascularization was measured and used for evaluation.

Downloaded from molpharm.aspetjournals.org at ASPET Journals on April 19, 2024

Molecular Pharmacology Fast Forward. Published on May 20, 2015 as DOI: 10.1124/mol.114.097345
This article has not been copyedited and formatted. The final version may differ from this version.

Results

SRPK1 inhibition potently suppresses VEGF production

Our previous report showed that SRPIN340 suppressed the level of VEGF mRNA in mouse retina (Dong et al., 2013). Gammons et al. reported that VEGF production was decreased in the human skin melanoma cells (A375) infected with a lentivirus containing *SRPK1* shRNA (Gammons et al., 2014). To confirm that inhibition of SRPK1 suppresses production of VEGF, we performed siRNA-mediated knockdown of *SRPK1* in the human retinal pigment epithelial cell line ARPE-19 (Supplemental Fig 1A). *VEGF* mRNA expression and secreted VEGF protein in culture supernatants were measured by RT-qPCR and ELISA, respectively. siRNA against the *luciferase* gene was used as a negative control. Treatment with siRNA against *SRPK1* suppressed the level of *VEGF* mRNA to 53% of the control ($p < 0.01$, Supplemental Fig 1B) and decreased the level of secreted VEGF protein to 36% of the control ($p < 0.01$, Supplemental Fig 1C). These results are consistent with previous studies showing that SRPIN340 suppresses VEGF production (Dong et al., 2013), and validated our strategy of targeting SRPK1 to develop novel anti-angiogenic treatments.

Downloaded from molpharm.aspetjournals.org at ASPET Journals on April 19, 2024

Molecular Pharmacology Fast Forward. Published on May 20, 2015 as DOI: 10.1124/mol.114.097345
This article has not been copyedited and formatted. The final version may differ from this version.

Crystal structure of SRPK1 bound with SRPIN340

Structural information about the binding mode of SRPIN340 in the ATP-binding pocket of SRPK1 will facilitate development of a new class of SRPK1 inhibitors. Hence, we co-crystalized the SRPK1/SRPIN340 complex and determined its structure by X-ray crystallography. Recombinant SRPK1 kinase domain was produced in *E. coli* and purified by immobilized nickel-chelate affinity chromatography, followed by gel-filtration chromatography. The crystals of SRPK1 was obtained from the purified protein and then soaked in a buffer containing SRPIN340. The X-ray crystallographic data are summarized in Supplemental Table 1. The crystallographic structure of the SRPK1/SRPIN340 complex is shown in Fig 1A (PDB ID: 4WUA). SRPIN340 binds SRPK1 at the ATP-binding cleft and forms extensive hydrophobic interactions with residues including Leu86, Val94, Phe165, Leu168, Leu220, Tyr231, and Leu231 (Fig 1B). The oxygen atom of the carbonyl group of SRPIN340 fixes the position of the ligand by forming a hydrogen bond with the main-chain amide of Leu168 (Fig 1B). Compared with the crystal structure of unliganded SRPK1 (PDB ID: 1WAK), the Leu168–Gly169

Downloaded from molpharm.aspetjournals.org at ASPET Journals on April 19, 2024

Molecular Pharmacology Fast Forward. Published on May 20, 2015 as DOI: 10.1124/mol.114.097345
This article has not been copyedited and formatted. The final version may differ from this version.

peptide was flipped in the SRPK1/SRPIN340 complex (Fig 1C), suggesting that peptide flipping was induced by the binding of SRPIN340 in the ATP-binding pocket. The trifluoromethyl group of SRPIN340 is located in the region occupied by the main-chain oxygen of Leu168 in the unliganded SRPK1 structure (Fig 1C), suggesting that the bulky trifluoromethyl group pushes away the main chain of Leu168 and induces peptide flipping. Furthermore, the flipped main-chain oxygen of Leu168 forms a hydrogen bond with the main-chain nitrogen of Val223 (Fig 1C), potentially stabilizing the flipped structure. These results demonstrate that SRPIN340 binds to the ATP-binding pocket and induces peptide flipping, which is probably required for potent inhibition of SRPK1.

In silico and subsequent *in vitro* screening of chemical inhibitors of SRPK1

To identify a new class of SRPK1 inhibitors, we screened a chemical library containing 71,955 chemical structures. Specifically, we performed a sequential screen consisting of an *in silico* docking study following by a pharmacophore search or similarity search of known inhibitors of CMGC family kinases, and selected the top 9,511 compounds. These chemical compounds were then assessed by *in vitro* kinase assay using recombinant

Downloaded from molpharm.aspetjournals.org at ASPET Journals on April 19, 2024

Molecular Pharmacology Fast Forward. Published on May 20, 2015 as DOI: 10.1124/mol.114.097345
This article has not been copyedited and formatted. The final version may differ from this version.

SRPK1 and its substrate. A summary of the *in vitro* screening results is provided in Fig 2A. We selected the top three compounds that inhibit SRPK1 activity to <10% of the DMSO control. Two of these compounds possess scaffolds found in frequent hitters (Baell and Holloway, 2010), and were consequently omitted. Thus, the strongest inhibitor was named SRPIN803 (Fig 2B). SRPIN803 was re-synthesized (Supplemental Information), and its activity and specificity were confirmed by *in vitro* kinase assay: the compound inhibited the *in vitro* activity of SRPK1 with an IC_{50} value of 2.4 μM, but did not inhibit SRPK2 (Fig 2C).

To predict the binding mode of SRPIN803 to the ATP-binding pocket of SRPK1, we performed an *in silico* docking study. The simulation revealed that SRPIN803 interacts with the ATP-binding pocket, and that the trifluoromethyl group of SRPIN803 was located in the same region as in the SRPIN340/SRPK1 crystal structure (Fig 2D).

SRPIN803 suppresses VEGF production

In the next step, we investigated whether SRPIN803 suppressed the VEGF production in

Downloaded from molpharm.aspetjournals.org at ASPET Journals on April 19, 2024

Molecular Pharmacology Fast Forward. Published on May 20, 2015 as DOI: 10.1124/mol.114.097345
This article has not been copyedited and formatted. The final version may differ from this version.

ARPE-19 cells. As we expected, treatment with SRPIN803 (10 μM) for 24 hours decreased the level of secreted VEGF protein in the culture supernatant, relative to treatment with 0.1% DMSO ($p < 0.01$; Fig 3A), with no cytotoxicity (Supplemental Fig 2). In addition, treatment with SRPIN803 (10 μM) significantly suppressed the expression of the *VEGF* mRNA to 48% of the control ($p < 0.01$, Fig 3B), suggesting that SRPIN803 inhibited the expression of *VEGF* mRNA. Furthermore, treatment with SRPIN803 suppressed the VEGF production in a dose and time-dependent manners (Supplemental Fig 3).

Next, we examined the effect of SRPIN803 on the transcriptome, using ARPE-19 cells treated with SRPIN803 (10 μM) for 4 hours. A summary of gene-expression array data is provided in Supplemental Fig 3 (GEO accession number: GSE62947, detailed data; Supplemental Table 2). mRNA levels of *VEGF* and 30 other genes were reduced by more than 1.8-fold (Supplemental Fig 4). The downregulated genes included *IL8*, *HMOX1*, and *HK2*, which play a role in angiogenesis (Dulak et al., 2008; Martin et al., 2009; Wolf et al., 2011). Thus, SRPIN803 regulates expression of genes involved in angiogenesis.

Downloaded from molpharm.aspetjournals.org at ASPET Journals on April 19, 2024

Molecular Pharmacology Fast Forward. Published on May 20, 2015 as DOI: 10.1124/mol.114.097345
This article has not been copyedited and formatted. The final version may differ from this version.

Structural requirement of SRPIN803

To confirm the structural requirements of SRPK1 inhibition by SRPIN803, we performed *in vitro* kinase assays and the VEGF secretion assays using four derivative compounds of SRPIN803 in which the trifluoromethyl group was replaced. Substitutions of the trifluoromethyl group decreased both the inhibitory activity of SRPK1 and the suppression of VEGF production (Fig 3C). These results demonstrated that the trifluoromethyl group of SRPIN803 plays a crucial role in both SRPK1 inhibition and the suppression of VEGF production. To further analyze the structural requirements for SRPK1 inhibition, we purchased the compounds which were structurally similar to SRPIN803 and retained the trifluoromethyl group, and checked their SRPK1 inhibition. Structures of these compounds and inhibitory activities against SRPK1 were summarized in Supplemental Table 3. The derivatives that possess similar R2 groups to SRPIN803 inhibited SRPK1, though their inhibitory activities were weaker compared to SRPIN803. In contrast, the derivatives with larger or structurally different R2 groups did not inhibit SRPK1, as predicted by the docking simulation.

Downloaded from molpharm.aspetjournals.org at ASPET Journals on April 19, 2024

Molecular Pharmacology Fast Forward. Published on May 20, 2015 as DOI: 10.1124/mol.114.097345
This article has not been copyedited and formatted. The final version may differ from this version.

SRPIN803 is a dual inhibitor of SRPK1 and CK2α1/2α2

To determine the kinase selectivity of SRPIN803, we assessed its inhibitory effect against a panel of 306 kinases. In these experiments, we used SRPIN803 at a concentration of 2.5 μM. Only two other kinases, CK2α1 and CK2α2, were inhibited by more than 50% (Fig 4A, Supplemental Table S3). CK2α1 and CK2α2 form a tetrameric complex that constitutes the catalytic subunit of CK2 (Hathaway and Traugh, 1982; Meisner et al., 1989; Pinna, 1990). In the following experiments, we used the tetrameric complex of CK2. In the *in vitro* kinase assay, the IC_{50} value of SRPIN803 against CK2 was 203 nM (Fig 4B). Thus, SRPIN803 is a dual inhibitor of SRPK1 and CK2. By contrast, SRPIN340 did not inhibit CK2 (Fig 4B), suggesting that CK2 is also involved in the effective inhibition of VEGF production.

To verify inhibition of CK2 by SRPIN803, we performed an *in silico* docking simulation using the crystal structure of CK2α (PDB ID: 1M2Q). The simulation revealed that SRPIN803 fits into the ATP-binding pocket of CK2α (Fig 4C), while SRPIN340 does not fit (Supplemental Fig 5), supporting the idea that SRPIN803 is the

Downloaded from molpharm.aspetjournals.org at ASPET Journals on April 19, 2024

Molecular Pharmacology Fast Forward. Published on May 20, 2015 as DOI: 10.1124/mol.114.097345
This article has not been copyedited and formatted. The final version may differ from this version.

dual inhibitor of SRPK1 and CK2α.

CK2 plays a role in the VEGF production

CK2 is a ubiquitous serine/threonine kinase that phosphorylates and/or interacts with more than 300 substrates (Meggio and Pinna, 2003), and is involved in many central biological processes (Litchfield, 2003; Olsten and Litchfield, 2004; Unger et al., 2004), including VEGF production (Noy et al., 2012a; Noy et al., 2012b). Three inhibitors of CK2, DRB, TBB, and apigenin, as well as overexpression of a dominant-negative mutant of CK2α, inhibit hypoxia-inducible factor-1 (HIF1) activity and consequently prevent induction of VEGF expression by hypoxia (Mottet et al., 2005).

To investigate whether CK2 inhibition contributes to reduction of the VEGF production, we performed siRNA-mediated knockdown of *CK2A1* and *CK2A2* in ARPE-19 cells (Fig 4D). Treatment with siRNA against either *CK2A1* or *CK2A2* significantly suppressed the expression of *VEGF* mRNA (Fig 4E), and decreased the level of secreted VEGF protein (Fig 4F), relative to the control. Furthermore, knockdown of both *CK2A1* and *CK2A2* increased the suppression of VEGF expression and secretion

Downloaded from molpharm.aspetjournals.org at ASPET Journals on April 19, 2024

Molecular Pharmacology Fast Forward. Published on May 20, 2015 as DOI: 10.1124/mol.114.097345
This article has not been copyedited and formatted. The final version may differ from this version.

(Fig 4E and 4F). Thus, CK2 is also involved in VEGF production. Furthermore, the level of secreted VEGF protein was not significantly reduced by SRPIN803 in the co-depleted cells of SRPK and CK2, relative to the control (Supplemental Fig 6). Taken together, these findings indicate that the antiangiogenic effect of SPRIN803 is mediated by the dual inhibition of SRPK1 and CK2.

Intravitreous injection of SRPIN803

Based on the potent anti-VEGF activity of SRPIN803, we investigated whether SRPIN803 is an effective anti-angiogenic drug in a mouse model. We performed laser photocoagulation to cause pathological choroidal neovascularization beneath the retina, thereby generating a mouse model that recapitulates the pathogenesis of AMD (Aguilar et al., 2008). Just after the laser photocoagulation, we injected SRPIN803 once intravitreously. Seven days later, FITC-dextran was injected into left ventricle, and the eyes were enucleated, opened by incision, and laid flat. The flat-mounts of the eyes were visualized by fluorescence microscopy, and the areas of neovascularization were quantitated. The injection of SRPIN803 significantly decreased the neovascularization

Downloaded from molpharm.aspetjournals.org at ASPET Journals on April 19, 2024

Molecular Pharmacology Fast Forward. Published on May 20, 2015 as DOI: 10.1124/mol.114.097345
This article has not been copyedited and formatted. The final version may differ from this version.

area, relative to DMSO injection ($p < 0.01$), in a dose-dependent manner (Fig 5A and 5B). SRPIN340 also decreased the area of neovascularization, but its activity was weaker than that of SRPIN803 (Supplemental Fig 7).

In order to confirm reduction of inflammation-associated molecules following treatment with SRPIN803, as previously reported for SRPIN340 (Aguilar et al., 2008; Dong et al., 2013), we measured the levels of monocyte chemoattractant protein-1 (MCP1) and intercellular adhesion molecule-1 (ICAM1) in retinal pigment epithelium and choroid 3 days after laser photocoagulation and intravitreous injection of SRPIN803. Expression levels of both MCP1 and ICAM1 were reduced by treatment with SRPIN803 (20 pmol/eye), relative to treatment with 0.1% DMSO (Fig 5C and 5D, $p < 0.05$). Thus, SRPIN803 suppressed both expression of inflammation-associated molecules and laser-induced neovascularization.

Treatment with eye ointment containing SRPIN803

Intravitreous injection increases the risk of multiple complications. Therefore, we developed an eye ointment containing SRPIN803 at a final concentration of 10%.

Downloaded from molpharm.aspetjournals.org at ASPET Journals on April 19, 2024

Molecular Pharmacology Fast Forward. Published on May 20, 2015 as DOI: 10.1124/mol.114.097345
This article has not been copyedited and formatted. The final version may differ from this version.

SRPIN803 was stable in the ointment for 4 weeks under various conditions (Supplemental Table 4). To determine whether topical administration of the ointment could suppress neovascularization, we administered it to model mice three times a day for 7 days after laser photocoagulation. Treatment with SRPIN803 ointment significantly decreased the neovascularization area, relative to treatment with substrate alone (Fig 6A and 6B, $p < 0.01$). These data demonstrate that SRPIN803 has therapeutic activity, even in a topical ointment.

Downloaded from molpharm.aspetjournals.org at ASPET Journals on April 19, 2024

Molecular Pharmacology Fast Forward. Published on May 20, 2015 as DOI: 10.1124/mol.114.097345
This article has not been copyedited and formatted. The final version may differ from this version.

Discussion

In this study, we solved the crystal structure of the SRPK1/SRPIN340 complex. The structure revealed that SRPIN340 binds to the ATP-binding pocket and induces peptide flipping. Based on the structural information, we screened a large-scale chemical library using an *in silico* virtual method followed by *in vitro* kinase assays. This screen identified SRPIN803, which was revealed to be a dual inhibitor of SRPK1 and CK2. The dual action of this drug efficiently suppressed VEGF production in the ARPE-19 cells. Furthermore, SRPIN803 suppressed choroidal neovascularization in model mice. Thus, SRPIN803 represents a promising candidate drug for treatment of neovascular diseases.

Peptide flipping induced by inhibitor binding to the pocket, which rearranges the hydrogen-bond network, has been demonstrated to enhance the inhibitor selectivity in mitogen-activated phosphatase and Tau-tubulin kinase 1 (Fitzgerald et al., 2003; Nolen et al., 2003; Xue et al., 2013). SRPIN340 also induced peptide flipping in the pocket, a process in which the trifluoromethyl group of SRPIN340 may be involved. SRPIN803 also contains a trifluoromethyl group, positioned similarly to that in the SRPK1/SRPIN340 complex, indicating that the trifluoromethyl group plays a critical role

Downloaded from molpharm.aspetjournals.org at ASPET Journals on April 19, 2024

Molecular Pharmacology Fast Forward. Published on May 20, 2015 as DOI: 10.1124/mol.114.097345
This article has not been copyedited and formatted. The final version may differ from this version.

in selective inhibition of SRPK1. Data obtained using structural derivatives of SRPIN803 in which the trifluoromethyl group was replaced support the significance of this moiety to the drug's inhibitory activity.

Our group and others previously reported that SRPIN340 suppresses retinal neovascularization (Gammons et al., 2013; Nowak et al., 2010) and choroidal neovascularization (Dong et al., 2013) in model mice and rats. Furthermore, SRPIN340 and siRNA-mediated knockdown of *SRPK1* reduced VEGF-mediated tumor angiogenesis in metastatic melanoma (Gammons et al., 2014). In this study, we showed that the siRNA-mediated knockdown of *SRPK1* inhibited VEGF production, and that SRPIN803 suppressed choroidal neovascularization in model mice. Taken together, these data strongly support the idea that SRPK1 is a potential target for treatment of pathological angiogenesis.

We showed previously that SRPIN340 suppressed *VEGF* mRNA expression in model mice (Dong et al., 2013). Here, we showed that *VEGF* mRNA expression was decreased in the ARPE-19 cells by either knockdown (si*SRPK1*) or treatment with SRPIN803. SRPIN803 inhibited not only SRPK1 but also CK2, an important regulator of

Downloaded from molpharm.aspetjournals.org at ASPET Journals on April 19, 2024

Molecular Pharmacology Fast Forward. Published on May 20, 2015 as DOI: 10.1124/mol.114.097345
This article has not been copyedited and formatted. The final version may differ from this version.

HIF1 activity that activates transcription of the VEGF gene (Mottet et al., 2005). Inhibitors of CK2 decrease VEGF production in retinal pigmental epithelial cells (Mottet et al., 2005; Pollreisz et al., 2013), suppress proliferation and migration of retinal endothelial cells (Ljubimov et al., 2004), and decrease retinal neovascularization in mouse models of oxygen-induced retinopathy (Kramerov et al., 2008) and endometriotic lesions (Feng et al., 2012). Furthermore, siRNA-mediated knockdown of *CK2* decreased *VEGF* mRNA expression and VEGF protein level. Intravitreous injection of SRPIN803 suppressed choroidal neovascularization in model mice more effectively than SRPIN340, whereas the inhibitory activity of SRPIN803 against SRPK1 was weaker than that of SRPIN340. Because SRPIN340 did not inhibit CK2, this observation can be attributed to the dual inhibitory activity of SRPIN803.

This study indicated that VEGF production was decreased in the ARPE-19 cells transfected siRNAs of either *SRPK1* or *CK2*, and SRPIN803 decreased VEGF production through the inhibition of SRPK1 and/or CK2. Mylonis et al. reported that CK2 phosphorylated and activated SRPK1 (Mylonis and Giannakouros, 2003). It has been unknown whether these two kinases are involved in the regulation of VEGF

Downloaded from molpharm.aspetjournals.org at ASPET Journals on April 19, 2024

Molecular Pharmacology Fast Forward. Published on May 20, 2015 as DOI: 10.1124/mol.114.097345
This article has not been copyedited and formatted. The final version may differ from this version.

production independently or not. Thus, further studies are required to understand how CK2 and SRPK1 regulate the VEGF production.

Previous studies reported that repeated intravitreous injection of anti-VEGF drugs is associated with reduced bioefficacy (Schaal et al., 2008), and visual acuity has decreased in several percent of patients treated with existing anti-VEGF therapies (Comparison of Age-related Macular Degeneration Treatments Trials Research et al., 2012). One potential explanation for this is that the density of macrophages was higher in regions of choroidal neovascularization treated with anti-VEGF antibody than in the absence of treatment (Tatar et al., 2008). Macrophages express VEGF within the choroidal neovascularization (Grossniklaus et al., 2002), and this expression is related to the severity of choroidal neovascularization (Espinosa-Heidmann et al., 2003; Sakurai et al., 2003). In this study, SRPIN803 reduced the protein level of MCP1, which plays a role in macrophage recruitment (Salcedo et al., 2000). Thus, MCP1 suppression by SRPIN803 may contribute to the drug's potent *in vivo* effect.

This study identified a dual inhibitor of SRPK1 and CK2, SRPIN803, as a potential drug candidate for therapies against of neovascular diseases. Treatment with

Downloaded from molpharm.aspetjournals.org at ASPET Journals on April 19, 2024

Molecular Pharmacology Fast Forward. Published on May 20, 2015 as DOI: 10.1124/mol.114.097345
This article has not been copyedited and formatted. The final version may differ from this version.

SRPIN803 did not cause any cytotoxicity in ARPE-19 cells. Furthermore, administration of the drug either by intravitreous injection or as a topical ointment suppressed choroidal neovascularization in the model mice. In AMD patients, the route of administration for anti-VEGF antibodies is limited to intravitreous injection, which imposes a burden on both patients and doctors because of the elevated risk of several complications. Our findings suggest that SRPIN803 could contribute to avoidance of this risk.

Anti-VEGF antibodies have also been approved not only for other intraocular neovascular diseases, such as retinal vein occlusion and diabetic retinopathy, but also for various cancers, including colorectal cancer, lung cancer, and glioblastoma. It is possible that SRPIN803 could have an effect on these neovascular diseases. Overall, the findings reported here indicate that SRPIN803 represents a novel anti-VEGF agent for use in clinical therapeutics.

Downloaded from molpharm.aspetjournals.org at ASPET Journals on April 19, 2024

Molecular Pharmacology Fast Forward. Published on May 20, 2015 as DOI: 10.1124/mol.114.097345
This article has not been copyedited and formatted. The final version may differ from this version.

Acknowledgements

We thank Souhei Matsushita (Tokyo Medical and Dental University) for crystal structure analyses, and Manami Sasaki (Kyoto University), Sayaka Matsumura (Kyoto University), and Dr. Kenji Suda (Kyoto University) for technical assistance. We also thank the Institute of Laboratory Animals of Kyoto University for critical assistance with animal experiments, and the Radioisotope Research Center of Kyoto University for critical assistance with the radioisotope experiments.

Downloaded from molpharm.aspetjournals.org at ASPET Journals on April 19, 2024

Molecular Pharmacology Fast Forward. Published on May 20, 2015 as DOI: 10.1124/mol.114.097345
This article has not been copyedited and formatted. The final version may differ from this version.

Authorship Contributions

Participated in research design: Morooka, Kii, Yoshimura, and Hagiwara

Conducted experiments: Morooka, Denawa, Ninomiya, Fukuhara, Noda, and Ishida

*Contributed new reagents or analytic tool*s: Hoshina, Okabe, Kojima, Inoue, Okuno, Ikura, Furuya, and Nagano, Hosoya, and Ito.

Performed data analysis: Morooka, and Denawa

Wrote or contributed to the writing of the manuscript: Morooka, Kii, Hosoya, Ito, and Hagiwara.

Downloaded from molpharm.aspetjournals.org at ASPET Journals on April 19, 2024

Molecular Pharmacology Fast Forward. Published on May 20, 2015 as DOI: 10.1124/mol.114.097345
This article has not been copyedited and formatted. The final version may differ from this version.

References

Aguilar E, Dorrell MI, Friedlander D, Jacobson RA, Johnson A, Marchetti V, Moreno SK, Ritter MR and Friedlander M (2008) Chapter 6. Ocular models of angiogenesis. *Methods in enzymology* **444**: 115-158.

Amin EM, Oltean S, Hua J, Gammons MV, Hamdollah-Zadeh M, Welsh GI, Cheung MK, Ni L, Kase S, Rennel ES, Symonds KE, Nowak DG, Royer-Pokora B, Saleem MA, Hagiwara M, Schumacher VA, Harper SJ, Hinton DR, Bates DO and Ladomery MR (2011) WT1 mutants reveal SRPK1 to be a downstream angiogenesis target by altering VEGF splicing. *Cancer cell* **20**(6): 768-780.

Baell JB and Holloway GA (2010) New substructure filters for removal of pan assay interference compounds (PAINS) from screening libraries and for their exclusion in bioassays. *Journal of medicinal chemistry* **53**(7): 2719-2740.

Comparison of Age-related Macular Degeneration Treatments Trials Research G, Martin DF, Maguire MG, Fine SL, Ying GS, Jaffe GJ, Grunwald JE, Toth C, Redford M and Ferris FL, 3rd (2012) Ranibizumab and bevacizumab for treatment of neovascular age-related macular degeneration: two-year results. *Ophthalmology* **119**(7): 1388-1398.

Daub H, Blencke S, Habenberger P, Kurtenbach A, Dennenmoser J, Wissing J, Ullrich A and Cotten M (2002) Identification of SRPK1 and SRPK2 as the major cellular protein kinases phosphorylating hepatitis B virus core protein. *Journal of virology* **76**(16): 8124-8137.

De Moliner E, Moro S, Sarno S, Zagotto G, Zanotti G, Pinna LA and Battistutta R (2003) Inhibition of protein kinase CK2 by anthraquinone-related compounds. A structural insight. *The Journal of biological chemistry* **278**(3): 1831-1836.

Dong Z, Noda K, Kanda A, Fukuhara J, Ando R, Murata M, Saito W, Hagiwara M and Ishida S (2013) Specific inhibition of serine/arginine-rich protein kinase attenuates choroidal neovascularization. *Molecular vision* **19**: 536-543.

Dulak J, Deshane J, Jozkowicz A and Agarwal A (2008) Heme oxygenase-1 and carbon monoxide in vascular pathobiology: focus on angiogenesis. *Circulation* **117**(2): 231-241.

Emsley P, Lohkamp B, Scott WG and Cowtan K (2010) Features and development of Coot. *Acta crystallographica Section D, Biological crystallography* **66**(Pt 4):

Downloaded from molpharm.aspetjournals.org at ASPET Journals on April 19, 2024

Molecular Pharmacology Fast Forward. Published on May 20, 2015 as DOI: 10.1124/mol.114.097345
This article has not been copyedited and formatted. The final version may differ from this version.

486-501.

Espinosa-Heidmann DG, Suner IJ, Hernandez EP, Monroy D, Csaky KG and Cousins SW (2003) Macrophage depletion diminishes lesion size and severity in experimental choroidal neovascularization. *Investigative ophthalmology & visual science* **44**(8): 3586-3592.

Feng D, Welker S, Korbel C, Rudzitis-Auth J, Menger MD, Montenarh M and Laschke MW (2012) Protein kinase CK2 is a regulator of angiogenesis in endometriotic lesions. *Angiogenesis* **15**(2): 243-252.

Ferrara N, Gerber HP and LeCouter J (2003) The biology of VEGF and its receptors. *Nature medicine* **9**(6): 669-676.

Ferris FL, 3rd, Fine SL and Hyman L (1984) Age-related macular degeneration and blindness due to neovascular maculopathy. *Archives of ophthalmology* **102**(11): 1640-1642.

Fitzgerald CE, Patel SB, Becker JW, Cameron PM, Zaller D, Pikounis VB, O'Keefe SJ and Scapin G (2003) Structural basis for p38alpha MAP kinase quinazolinone and pyridol-pyrimidine inhibitor specificity. *Nature structural biology* **10**(9): 764-769.

Fukuda R, Hirota K, Fan F, Jung YD, Ellis LM and Semenza GL (2002) Insulin-like growth factor 1 induces hypoxia-inducible factor 1-mediated vascular endothelial growth factor expression, which is dependent on MAP kinase and phosphatidylinositol 3-kinase signaling in colon cancer cells. *The Journal of biological chemistry* **277**(41): 38205-38211.

Fukuhara T, Hosoya T, Shimizu S, Sumi K, Oshiro T, Yoshinaka Y, Suzuki M, Yamamoto N, Herzenberg LA, Herzenberg LA and Hagiwara M (2006) Utilization of host SR protein kinases and RNA-splicing machinery during viral replication. *Proceedings of the National Academy of Sciences of the United States of America* **103**(30): 11329-11333.

Gammons MV, Dick AD, Harper SJ and Bates DO (2013) SRPK1 inhibition modulates VEGF splicing to reduce pathological neovascularization in a rat model of retinopathy of prematurity. *Investigative ophthalmology & visual science* **54**(8): 5797-5806.

Gammons MV, Lucas R, Dean R, Coupland SE, Oltean S and Bates DO (2014) Targeting SRPK1 to control VEGF-mediated tumour angiogenesis in metastatic melanoma.

Downloaded from molpharm.aspetjournals.org at ASPET Journals on April 19, 2024

Molecular Pharmacology Fast Forward. Published on May 20, 2015 as DOI: 10.1124/mol.114.097345
This article has not been copyedited and formatted. The final version may differ from this version.

British journal of cancer **111**(3): 477-485.

Gragoudas ES, Adamis AP, Cunningham ET, Jr., Feinsod M, Guyer DR and Group VISiONCT (2004) Pegaptanib for neovascular age-related macular degeneration. *The New England journal of medicine* **351**(27): 2805-2816.

Grossniklaus HE, Ling JX, Wallace TM, Dithmar S, Lawson DH, Cohen C, Elner VM, Elner SG and Sternberg P, Jr. (2002) Macrophage and retinal pigment epithelium expression of angiogenic cytokines in choroidal neovascularization. *Molecular vision* **8**: 119-126.

Hathaway GM and Traugh JA (1982) Casein kinases--multipotential protein kinases. *Current topics in cellular regulation* **21**: 101-127.

Heier JS, Brown DM, Chong V, Korobelnik JF, Kaiser PK, Nguyen QD, Kirchhof B, Ho A, Ogura Y, Yancopoulos GD, Stahl N, Vitti R, Berliner AJ, Soo Y, Anderesi M, Groetzbach G, Sommerauer B, Sandbrink R, Simader C, Schmidt-Erfurth U, View and Groups VS (2012) Intravitreal aflibercept (VEGF trap-eye) in wet age-related macular degeneration. *Ophthalmology* **119**(12): 2537-2548.

Hu SI, Katz M, Chin S, Qi X, Cruz J, Ibebunjo C, Zhao S, Chen A and Glass DJ (2012) MNK2 inhibits eIF4G activation through a pathway involving serine-arginine-rich protein kinase in skeletal muscle. *Science signaling* **5**(211): ra14.

Hurwitz H, Fehrenbacher L, Novotny W, Cartwright T, Hainsworth J, Heim W, Berlin J, Baron A, Griffing S, Holmgren E, Ferrara N, Fyfe G, Rogers B, Ross R and Kabbinavar F (2004) Bevacizumab plus irinotecan, fluorouracil, and leucovorin for metastatic colorectal cancer. *The New England journal of medicine* **350**(23): 2335-2342.

Klein R, Wang Q, Klein BE, Moss SE and Meuer SM (1995) The relationship of age-related maculopathy, cataract, and glaucoma to visual acuity. *Investigative ophthalmology & visual science* **36**(1): 182-191.

Kramerov AA, Saghizadeh M, Caballero S, Shaw LC, Li Calzi S, Bretner M, Montenarh M, Pinna LA, Grant MB and Ljubimov AV (2008) Inhibition of protein kinase CK2 suppresses angiogenesis and hematopoietic stem cell recruitment to retinal neovascularization sites. *Molecular and cellular biochemistry* **316**(1-2): 177-186.

Lin J, Handschin C and Spiegelman BM (2005) Metabolic control through the PGC-1 family of transcription coactivators. *Cell metabolism* **1**(6): 361-370.

Downloaded from molpharm.aspetjournals.org at ASPET Journals on April 19, 2024

Molecular Pharmacology Fast Forward. Published on May 20, 2015 as DOI: 10.1124/mol.114.097345
This article has not been copyedited and formatted. The final version may differ from this version.

Litchfield DW (2003) Protein kinase CK2: structure, regulation and role in cellular decisions of life and death. *The Biochemical journal* **369**(Pt 1): 1-15.

Ljubimov AV, Caballero S, Aoki AM, Pinna LA, Grant MB and Castellon R (2004) Involvement of protein kinase CK2 in angiogenesis and retinal neovascularization. *Investigative ophthalmology & visual science* **45**(12): 4583-4591.

Maharaj AS and D'Amore PA (2007) Roles for VEGF in the adult. *Microvascular research* **74**(2-3): 100-113.

Martin D, Galisteo R and Gutkind JS (2009) CXCL8/IL8 stimulates vascular endothelial growth factor (VEGF) expression and the autocrine activation of VEGFR2 in endothelial cells by activating NFkappaB through the CBM (Carma3/Bcl10/Malt1) complex. *The Journal of biological chemistry* **284**(10): 6038-6042.

Meggio F and Pinna LA (2003) One-thousand-and-one substrates of protein kinase CK2? *FASEB journal : official publication of the Federation of American Societies for Experimental Biology* **17**(3): 349-368.

Meisner H, Heller-Harrison R, Buxton J and Czech MP (1989) Molecular cloning of the human casein kinase II alpha subunit. *Biochemistry* **28**(9): 4072-4076.

Mottet D, Ruys SP, Demazy C, Raes M and Michiels C (2005) Role for casein kinase 2 in the regulation of HIF-1 activity. *International journal of cancer Journal international du cancer* **117**(5): 764-774.

Murshudov GN, Skubak P, Lebedev AA, Pannu NS, Steiner RA, Nicholls RA, Winn MD, Long F and Vagin AA (2011) REFMAC5 for the refinement of macromolecular crystal structures. *Acta crystallographica Section D, Biological crystallography* **67**(Pt 4): 355-367.

Mylonis I and Giannakouros T (2003) Protein kinase CK2 phosphorylates and activates the SR protein-specific kinase 1. *Biochemical and biophysical research communications* **301**(3): 650-656.

Ngo JC, Chakrabarti S, Ding JH, Velazquez-Dones A, Nolen B, Aubol BE, Adams JA, Fu XD and Ghosh G (2005) Interplay between SRPK and Clk/Sty kinases in phosphorylation of the splicing factor ASF/SF2 is regulated by a docking motif in ASF/SF2. *Molecular cell* **20**(1): 77-89.

Ngo JC, Gullingsrud J, Giang K, Yeh MJ, Fu XD, Adams JA, McCammon JA and Ghosh G (2007) SR protein kinase 1 is resilient to inactivation. *Structure* **15**(1): 123-133.

Downloaded from molpharm.aspetjournals.org at ASPET Journals on April 19, 2024

Molecular Pharmacology Fast Forward. Published on May 20, 2015 as DOI: 10.1124/mol.114.097345
This article has not been copyedited and formatted. The final version may differ from this version.

Nikolakaki E, Drosou V, Sanidas I, Peidis P, Papamarcaki T, Iakoucheva LM and Giannakouros T (2008) RNA association or phosphorylation of the RS domain prevents aggregation of RS domain-containing proteins. *Biochimica et biophysica acta* **1780**(2): 214-225.

Nishida A, Kataoka N, Takeshima Y, Yagi M, Awano H, Ota M, Itoh K, Hagiwara M and Matsuo M (2011) Chemical treatment enhances skipping of a mutated exon in the dystrophin gene. *Nature communications* **2**: 308.

Nolen B, Ngo J, Chakrabarti S, Vu D, Adams JA and Ghosh G (2003) Nucleotide-induced conformational changes in the Saccharomyces cerevisiae SR protein kinase, Sky1p, revealed by X-ray crystallography. *Biochemistry* **42**(32): 9575-9585.

Nowak DG, Amin EM, Rennel ES, Hoareau-Aveilla C, Gammons M, Damodoran G, Hagiwara M, Harper SJ, Woolard J, Ladomery MR and Bates DO (2010) Regulation of vascular endothelial growth factor (VEGF) splicing from pro-angiogenic to anti-angiogenic isoforms: a novel therapeutic strategy for angiogenesis. *The Journal of biological chemistry* **285**(8): 5532-5540.

Noy P, Gaston K and Jayaraman PS (2012a) Dasatinib inhibits leukaemic cell survival by decreasing PRH/Hhex phosphorylation resulting in increased repression of VEGF signalling genes. *Leukemia research* **36**(11): 1434-1437.

Noy P, Sawasdichai A, Jayaraman PS and Gaston K (2012b) Protein kinase CK2 inactivates PRH/Hhex using multiple mechanisms to de-repress VEGF-signalling genes and promote cell survival. *Nucleic acids research* **40**(18): 9008-9020.

Ogawa Y and Hagiwara M (2012) Challenges to congenital genetic disorders with "RNA-targeting" chemical compounds. *Pharmacology & therapeutics* **134**(3): 298-305.

Okabe K, Kobayashi S, Yamada T, Kurihara T, Tai-Nagara I, Miyamoto T, Mukouyama Y-s, Sato Thomas N, Suda T, Ema M and Kubota Y (2014) Neurons Limit Angiogenesis by Titrating VEGF in Retina. *Cell* **159**(3): 584-596.

Olsten ME and Litchfield DW (2004) Order or chaos? An evaluation of the regulation of protein kinase CK2. *Biochemistry and cell biology = Biochimie et biologie cellulaire* **82**(6): 681-693.

Pinna LA (1990) Casein kinase 2: an 'eminence grise' in cellular regulation? *Biochimica et biophysica acta* **1054**(3): 267-284.

Pollreisz A, Afonyushkin T, Oskolkova OV, Gruber F, Bochkov VN and Schmidt-Erfurth

Downloaded from molpharm.aspetjournals.org at ASPET Journals on April 19, 2024

Molecular Pharmacology Fast Forward. Published on May 20, 2015 as DOI: 10.1124/mol.114.097345
This article has not been copyedited and formatted. The final version may differ from this version.

U (2013) Retinal pigment epithelium cells produce VEGF in response to oxidized phospholipids through mechanisms involving ATF4 and protein kinase CK2. *Experimental eye research* **116**: 177-184.

Rosenfeld PJ, Brown DM, Heier JS, Boyer DS, Kaiser PK, Chung CY, Kim RY and Group MS (2006) Ranibizumab for neovascular age-related macular degeneration. *The New England journal of medicine* **355**(14): 1419-1431.

Sakurai E, Anand A, Ambati BK, van Rooijen N and Ambati J (2003) Macrophage depletion inhibits experimental choroidal neovascularization. *Investigative ophthalmology & visual science* **44**(8): 3578-3585.

Salcedo R, Ponce ML, Young HA, Wasserman K, Ward JM, Kleinman HK, Oppenheim JJ and Murphy WJ (2000) Human endothelial cells express CCR2 and respond to MCP-1: direct role of MCP-1 in angiogenesis and tumor progression. *Blood* **96**(1): 34-40.

Schaal S, Kaplan HJ and Tezel TH (2008) Is there tachyphylaxis to intravitreal anti-vascular endothelial growth factor pharmacotherapy in age-related macular degeneration? *Ophthalmology* **115**(12): 2199-2205.

Seddon JM and Chen CA (2004) The epidemiology of age-related macular degeneration. *International ophthalmology clinics* **44**(4): 17-39.

Shima C, Sakaguchi H, Gomi F, Kamei M, Ikuno Y, Oshima Y, Sawa M, Tsujikawa M, Kusaka S and Tano Y (2008) Complications in patients after intravitreal injection of bevacizumab. *Acta ophthalmologica* **86**(4): 372-376.

Tatar O, Yoeruek E, Szurman P, Bartz-Schmidt KU, Tubingen Bevacizumab Study G, Adam A, Shinoda K, Eckardt C, Boeyden V, Claes C, Pertile G, Scharioth GB and Grisanti S (2008) Effect of bevacizumab on inflammation and proliferation in human choroidal neovascularization. *Archives of ophthalmology* **126**(6): 782-790.

Trott O and Olson AJ (2010) AutoDock Vina: improving the speed and accuracy of docking with a new scoring function, efficient optimization, and multithreading. *Journal of computational chemistry* **31**(2): 455-461.

Unger GM, Davis AT, Slaton JW and Ahmed K (2004) Protein kinase CK2 as regulator of cell survival: implications for cancer therapy. *Current cancer drug targets* **4**(1): 77-84.

Ventrice P, Leporini C, Aloe JF, Greco E, Leuzzi G, Marrazzo G, Scorcia GB, Bruzzichesi

Downloaded from molpharm.aspetjournals.org at ASPET Journals on April 19, 2024

Molecular Pharmacology Fast Forward. Published on May 20, 2015 as DOI: 10.1124/mol.114.097345
This article has not been copyedited and formatted. The final version may differ from this version.

D, Nicola V and Scorcia V (2013) Anti-vascular endothelial growth factor drugs safety and efficacy in ophthalmic diseases. *Journal of pharmacology & pharmacotherapeutics* **4**(Suppl 1): S38-42.

Wang P, Zhou Z, Hu A, Ponte de Albuquerque C, Zhou Y, Hong L, Sierecki E, Ajiro M, Kruhlak M, Harris C, Guan KL, Zheng ZM, Newton AC, Sun P, Zhou H and Fu XD (2014) Both decreased and increased SRPK1 levels promote cancer by interfering with PHLPP-mediated dephosphorylation of Akt. *Molecular cell* **54**(3): 378-391.

Winn MD, Ballard CC, Cowtan KD, Dodson EJ, Emsley P, Evans PR, Keegan RM, Krissinel EB, Leslie AG, McCoy A, McNicholas SJ, Murshudov GN, Pannu NS, Potterton EA, Powell HR, Read RJ, Vagin A and Wilson KS (2011) Overview of the CCP4 suite and current developments. *Acta crystallographica Section D, Biological crystallography* **67**(Pt 4): 235-242.

Wolf A, Agnihotri S, Micallef J, Mukherjee J, Sabha N, Cairns R, Hawkins C and Guha A (2011) Hexokinase 2 is a key mediator of aerobic glycolysis and promotes tumor growth in human glioblastoma multiforme. *The Journal of experimental medicine* **208**(2): 313-326.

Xu J, Liu X, Jiang Y, Chu L, Hao H, Liua Z, Verfaillie C, Zweier J, Gupta K and Liu Z (2008) MAPK/ERK signalling mediates VEGF-induced bone marrow stem cell differentiation into endothelial cell. *Journal of cellular and molecular medicine* **12**(6A): 2395-2406.

Xue Y, Wan PT, Hillertz P, Schweikart F, Zhao Y, Wissler L and Dekker N (2013) X-ray structural analysis of tau-tubulin kinase 1 and its interactions with small molecular inhibitors. *ChemMedChem* **8**(11): 1846-1854.

Downloaded from molpharm.aspetjournals.org at ASPET Journals on April 19, 2024

Molecular Pharmacology Fast Forward. Published on May 20, 2015 as DOI: 10.1124/mol.114.097345
This article has not been copyedited and formatted. The final version may differ from this version.

Footnotes

This work was supported by Target Protein Research Programs of the Ministry of Education, Culture, Sports, Science and Technology of Japan; Grants-in-Aid from the National Institute of Biochemical Innovation of Japan [Grants 12-03]; and Platform for Drug Discovery, Informatics, and Structural Life Science from the Ministry of Education, Culture, Sports, Science and Technology, Japan.

Downloaded from molpharm.aspetjournals.org at ASPET Journals on April 19, 2024

Molecular Pharmacology Fast Forward. Published on May 20, 2015 as DOI: 10.1124/mol.114.097345
This article has not been copyedited and formatted. The final version may differ from this version.

Figure Legends

Figure 1 Crystal structure of the SRPK1/SRPIN340 complex

(A) Overall structure. SRPK1 and SRPIN340 are shown in ribbon mode and stick mode, respectively. SRPIN340 binds to the ATP-binding pocket of SRPK1 (PDB ID: 4WUA).

(B) Stick representation of the inhibitor-binding site of the SRPK1/SRPIN340 complex. The red dotted line indicates a hydrogen bond. A space-filling model is illustrated by the dots surrounding the stick representation.

(C) The peptide flip around Leu168–Gly169. Residues Val164–His171 and Val223 are shown in stick representation. The structures illustrated are SRPK1 without ligand (PDB ID: 1WAK), shown in yellow, and SRPK1 with SRPIN340, shown in green. The red dotted line indicates a hydrogen bond.

Figure 2 Identification of SRPIN803 as an inhibitor of SRPK1

(A) Relative *in vitro* activities of SRPK1 in the presence of small molecules (10 μM). A total of 9,511 compounds were screened. The top three compounds that inhibited SRPK1 activity to below 10% of the DMSO control are shown in the scatter plot.

Downloaded from molpharm.aspetjournals.org at ASPET Journals on April 19, 2024

Molecular Pharmacology Fast Forward. Published on May 20, 2015 as DOI: 10.1124/mol.114.097345
This article has not been copyedited and formatted. The final version may differ from this version.

(B) Chemical structure referred to as SRPIN803.

(C) SRPIN803 inhibits the kinase activity of SRPK1 with an IC_{50} value of 2.4 μM, but does not inhibit SRPK2.

(D) A docking model for SRPIN803 to SRPK1 (right, Data Supplement 1), compared with the same view of the crystal structure of the SRPK1/SRPIN340 complex (left, PDB ID: 4WUA). The arrowhead indicates the trifluoromethyl group.

Figure 3 SRPIN803 suppresses VEGF production

(A and B) Treatment with SRPIN803 decreases total VEGF protein and *VEGF* mRNA relative to the treatment with 0.1% DMSO. *, $p < 0.01$. (A) ELISA of total VEGF protein in culture supernatants of ARPE-19 cells treated with SRPIN803 (10 μM) (mean ± SEM of four independent experiments). (B) Quantitative PCR analysis of total *VEGF* mRNA of the ARPE-19 cells treated with SRPIN803 (10 μM) (mean ± SEM of the results of four experiments performed in triplicate).

(C) Structural requirements for SRPK1 inhibition by SRPIN803. The chemical structures of SRPIN803 and its derivatives are shown. IC_{50} values of these derivatives were

Downloaded from molpharm.aspetjournals.org at ASPET Journals on April 19, 2024

Molecular Pharmacology Fast Forward. Published on May 20, 2015 as DOI: 10.1124/mol.114.097345
This article has not been copyedited and formatted. The final version may differ from this version.

calculated by *in vitro* kinase assay. The levels of secreted VEGF protein in culture supernatants of ARPE-19 cells treated with the derivatives (final concentration, 10 μM) were measured by ELISA.

Figure 4 SRPIN803 is a dual inhibitor of SRPK1 and CK2

(A) Scatter plots of the 306-kinase panel of SRPIN803 (2.5 μM). Black dots indicate greater than 50% inhibition.

(B) SRPIN803 inhibited CK2 activity with an IC_{50} value of 203 nM, whereas SRPIN340 did not inhibit the enzyme.

(C) A docking model of SRPIN803 bound to the ATP-binding pocket of CK2α (Data Supplement 2).

(D) Semiquantitative PCR analysis to determine expression of *CK2A1* and *CK2A2* in the ARPE-19 cells. siRNAs against *CK2A1* and *CK2A2* reduced the corresponding mRNA levels, relative to treatment with control siRNA against luciferase. *GAPDH* was used as an internal control.

(E and F) Treatment with siRNA against either *CK2A1* or *CK2A2* significantly

Downloaded from molpharm.aspetjournals.org at ASPET Journals on April 19, 2024

Molecular Pharmacology Fast Forward. Published on May 20, 2015 as DOI: 10.1124/mol.114.097345
This article has not been copyedited and formatted. The final version may differ from this version.

suppressed expression of *VEGF* mRNA and decreased the level of secreted VEGF protein, relative to the treatment with the control. *, $p < 0.01$. (E) Quantitative PCR analysis of total *VEGF* mRNA of the ARPE-19 cells transfected with siRNAs (means ± SEM of the results from four experiments performed in duplicate). (F) ELISA of secreted VEGF protein in the culture supernatants of the ARPE-19 cells transfected with siRNAs (means ± SEM of three independent experiments).

Figure 5 SRPIN803 suppresses choroidal neovascularization in laser-induced model mice

(A and B) Intravitreous injection of SRPIN803 suppressed choroidal neovascularization. (A) Choroidal flat mounts were prepared from model mice 7 days after laser photocoagulation combined with intravitreous injection of 0.1% DMSO or SRPIN803 (0.20 pmol, 2.0 pmol, 20 pmol). The areas of choroidal neovascularization lesions in the flat mounts were quantitated (means ± SEM, n (number of neovascular lesions) = 17–26; *, $p < 0.01$; **, $p < 0.05$; †, $p = 0.43$). (B) Representative micrographs of neovascular lesions prepared in A. Scale bar indicates 100 μm.

Downloaded from molpharm.aspetjournals.org at ASPET Journals on April 19, 2024

Molecular Pharmacology Fast Forward. Published on May 20, 2015 as DOI: 10.1124/mol.114.097345
This article has not been copyedited and formatted. The final version may differ from this version.

(C and D) Reduction of inflammatory molecules by injection of SRPIN803. Bars indicate average protein levels of MCP1 (C) and ICAM1 (D) in retinal pigment epithelium and choroid obtained from model mice 3 days after laser photocoagulation combined with intravitreous injection of 0.1% DMSO or SRPIN803 (20 pmol). Protein levels were measured with ELISA and normalized to total protein levels (means ± SEM, n (number of eyes) = 6; **, $p < 0.05$).

Figure 6 SRPIN803 ointment suppresses choroidal neovascularization

(A and B) Treatment with ointment containing SRPIN803 (final concentration, 10%) suppressed choroidal neovascularization. (A) Quantitative analysis of the area of neovascularization (means ± SEM, n (number of neovascular lesions) = 18 for the control, n = 26 for SRPIN803; *, $p < 0.01$). (B) Representative micrographs of neovascular lesions prepared in A. Scale bar indicates 100 μm.

Downloaded from molpharm.aspetjournals.org at ASPET Journals on April 19, 2024

Molecular Pharmacology Fast Forward. Published on May 20, 2015 as DOI: 10.1124/mol.114.097345
This article has not been copyedited and formatted. The final version may differ from this version.

(Data Supplement 1) A docking model for SRPIN803 to SRPK1 built from the crystal structure of human SRPK1 complexed to an inhibitor SRPIN340 (PDB ID: 4WUA).

(Data Supplement 2) A docking model of SRPIN803 bound to the ATP-binding pocket of CK2α built from the crystal structure of 1,8-di-hydroxy-4-nitro-xanten-9-one/CK2 kinase complex (PDB ID: 1M2Q(De Moliner et al., 2003)).

Downloaded from molpharm.aspetjournals.org at ASPET Journals on April 19, 2024

Figure 1

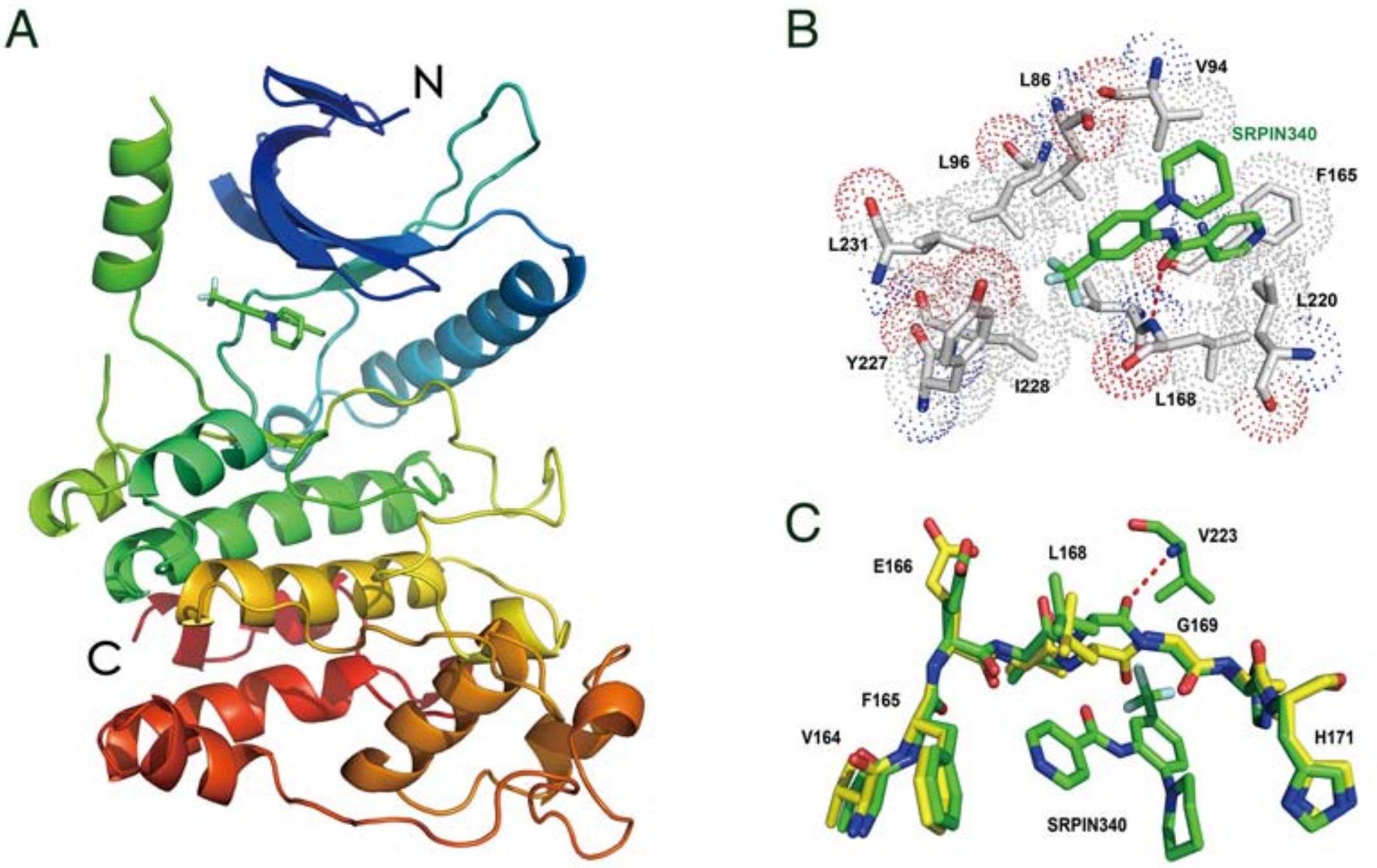
A
N
C
B
V94
L86
SRPIN340
L96
F165
L231
L220
Y227
I228
L168
C
V223
E166
L168
G169
F165
V164
H171
SRPIN340

Figure 2

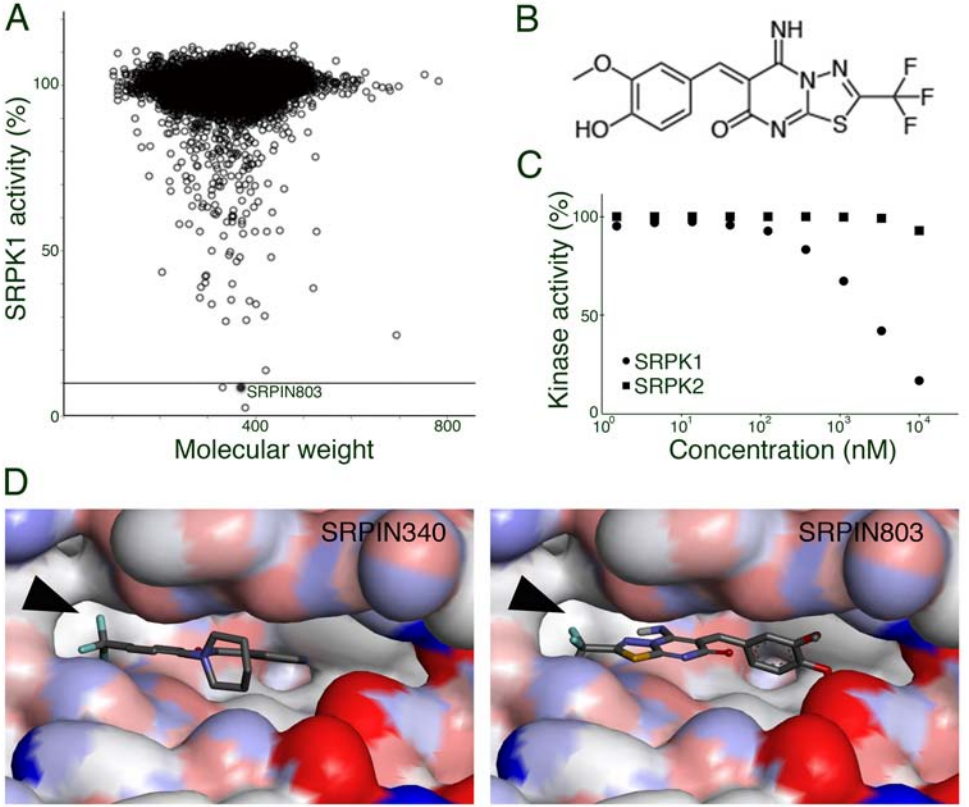
A
SRPK1 activity (%)
100
50
0
SRPIN803
400
800
Molecular weight
B
NH
O
HO
N
N
S
F
F
F
C
Kinase activity (%)
100
50
0
SRPK1
SRPK2
10^0
10^1
10^2
10^3
10^4
Concentration (nM)
D
SRPIN340
SRPIN803

Figure 3

A

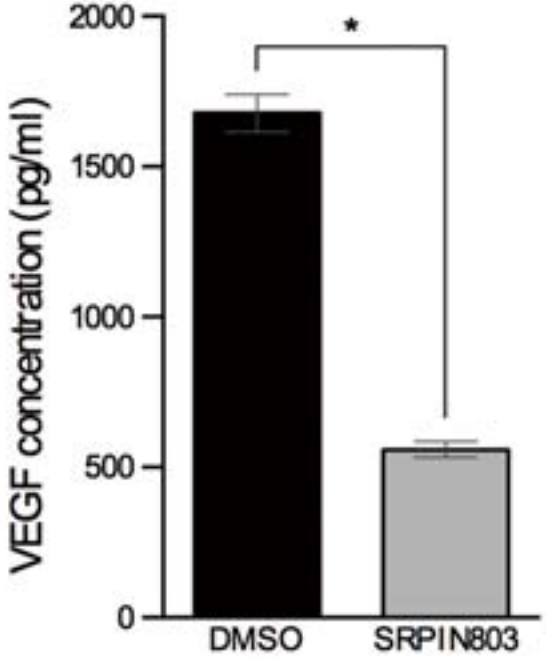

B

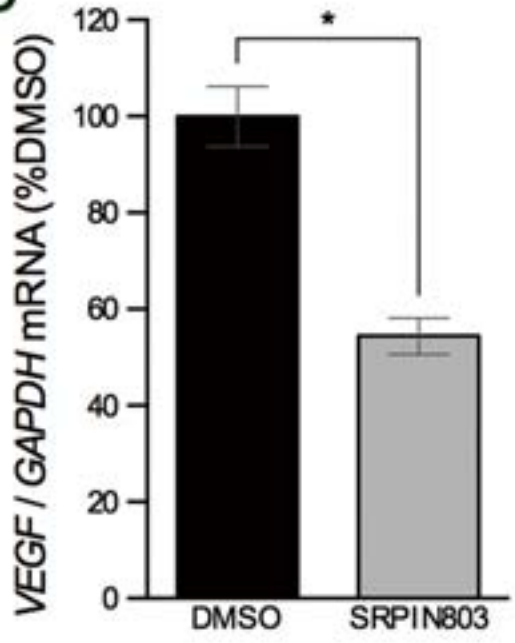

C

Compound No.		SRPIN803	SRPIN803a	SRPIN803b	SRPIN803c	SRPIN803d
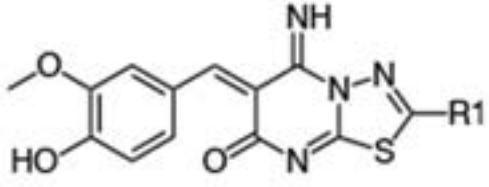	R1	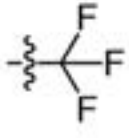	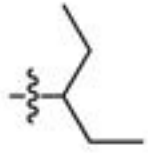	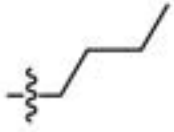		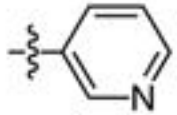
SRPK1 activity (%)		19.1	50.4	64.7	81.2	88.0
VEGF protein level compared with control (%)		28.1	54.3	88.6	76.1	93.9

Figure 4

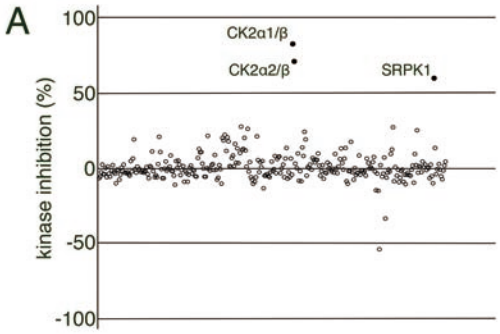
A
100
50
0
-50
-100
kinase inhibition (%)
CK2α1/β
CK2α2/β
SRPK1

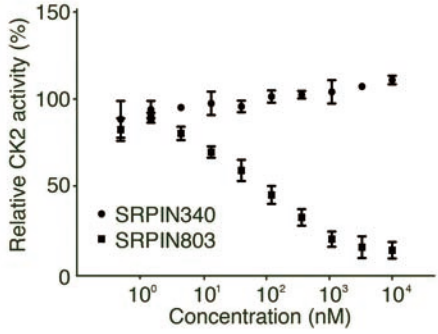
B
150
100
50
0
Relative CK2 activity (%)
SRPIN340
SRPIN803
10^0
10^1
10^2
10^3
10^4
Concentration (nM)

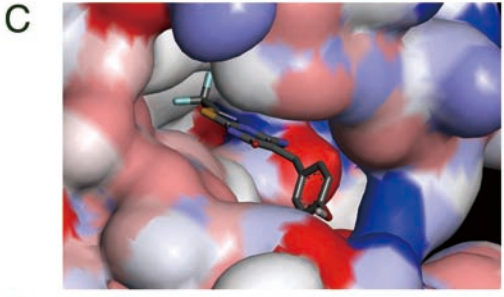
C

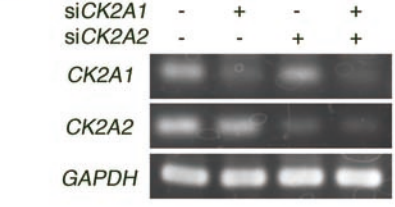
D
siCK2A1 - + - +
siCK2A2 - - + +
CK2A1
CK2A2
GAPDH

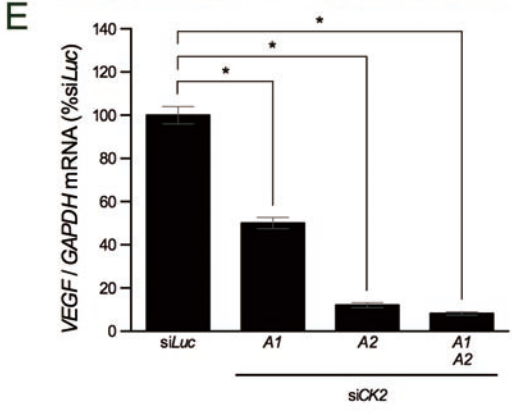
E
140
120
100
80
60
40
20
0
VEGF / GAPDH mRNA (%siLuc)
*
*
*
siLuc
A1
A2
A1
A2
siCK2

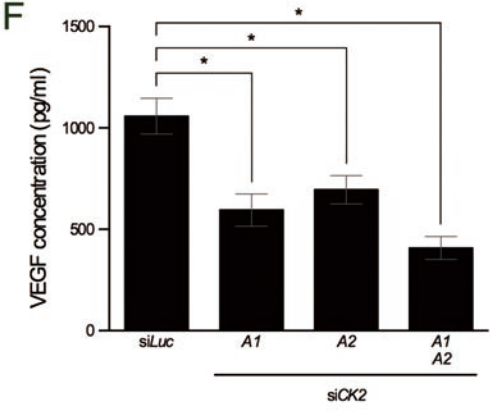
F
1500
1000
500
0
VEGF concentration (pg/ml)
*
*
*
siLuc
A1
A2
A1
A2
siCK2

Figure 5

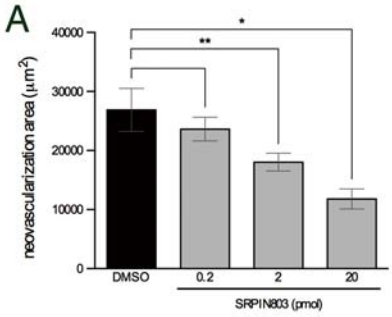
A
neovascularization area (μm²)
40000
30000
20000
10000
0
*
**
DMSO
0.2
2
20
SRPIN803 (pmol)

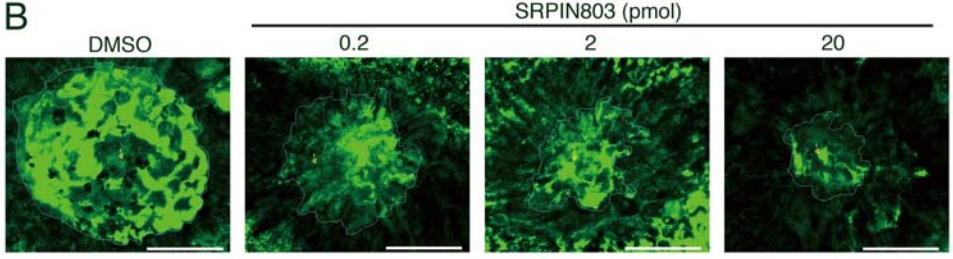
B
SRPIN803 (pmol)
DMSO
0.2
2
20

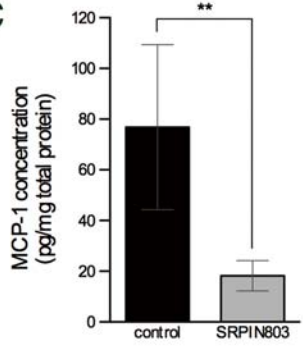
C
MCP-1 concentration (pg/mg total protein)
120
100
80
60
40
20
0
**
control
SRPIN803

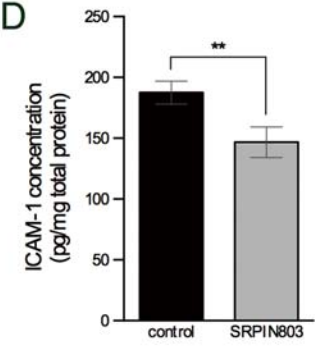
D
ICAM-1 concentration (pg/mg total protein)
250
200
150
100
50
0
**
control
SRPIN803

Figure 6

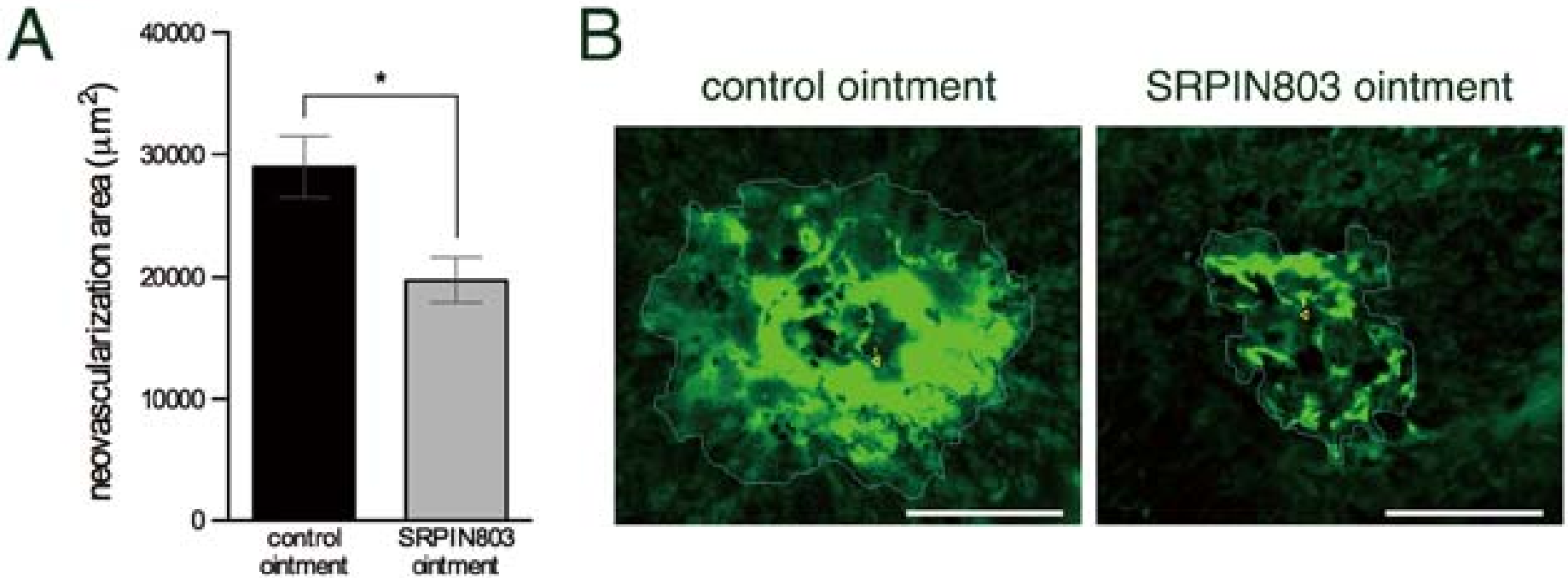
A
40000
30000
20000
10000
0
neovascularization area (μm²)
*
control ointment
SRPIN803 ointment
B
control ointment
SRPIN803 ointment